Dalton Transactions

PAPER

View Article Online
View Journal | View Issue

Cite this: *Dalton Trans.*, 2015, **44**, 733

Synthesis and magnetic properties of tartrate-bridging rare-earth-containing polytungstoarsenate aggregates from an adaptive precursor $[As_2W_{19}O_{67}(H_2O)]^{14-}$†

Yuan Wang,[a] Xiaopeng Sun,[a] Suzhi Li,[b] Pengtao Ma,[a] Jingping Wang*[a] and Jingyang Niu*[a]

Received 9th June 2014,
Accepted 4th November 2014

DOI: 10.1039/c4dt01703j

www.rsc.org/dalton

Six tartrate-bridging rare-earth-substituted polytungstoarsenates $[RE_2(C_4H_4O_6)(C_4H_2O_6)(As\ W_9O_{33})]_2^{18-}$ (Ho^{III} (**1**), Er^{III} (**2**), Tm^{III} (**3**), Yb^{III} (**4**), Lu^{III} (**5**), and Y^{III} (**6**)) have been synthesized under conventional solution conditions. They have been further characterized by elemental analyses, X-ray powder diffraction (XRPD), IR and UV-vis spectroscopy and single-crystal X-ray diffraction. Preliminary variable-temperature magnetic susceptibility measurements indicate that **1–4** exhibit antiferromagnetic coupling.

Introduction

Polyoxometalates (POMs), an important class of inorganic compounds displaying various compositional ranges and significant structural diversity,[1] have attracted increasing interest owing to their potential applications in different fields such as materials science,[2] medicine,[3] catalysis,[2] electrochemistry[4] and magnetic chemistry.[5] However, the formation mechanism of POMs is still not well understood and commonly described as self-assembly. Thus, the design of elaborate POMs remains a challenge. Generally speaking, two strategies, straightforward synthesis and a building block approach, have been developed to prepare novel POMs. It is considered that straightforward synthesis is a self-assembly process by which mononuclear oxoanions (like WO_4^{2-}, MoO_4^{2-}) aggregate into polynuclear POMs including the large and giant species at suitable pH.[6] Hitherto, many polynuclear POMs, such as tungstate $\{W_{148}\}$[7] and the largest molybdate $\{Mo_{368}\}$,[8] were obtained by a straightforward "one-pot" synthesis *via* the self-assembly process. However, the unpredictability and uncontrollability of the product confine its development. In contrast, the building block approach keeps expanding the arsenal of new POM-based complexes *via* step-by-step control of the aggregation process. It allows the chemists to fine-tune the reaction and create a large number of new compounds with purposeful actions. Therefore, the building block approach is deemed to be a more effective and feasible method to isolate the target product, especially for polyoxotungstates.[9] As for this strategy, vacant Keggin-type and Dawson-type polyoxoanions were extensively used as the building blocks and linked by metal cations in different ways to form various structural topologies from isolated clusters[9b,10] to chainlike aggregates.[11] Nevertheless, the dilacunary species $[As_2W_{19}O_{67}(H_2O)]^{14-}$ first draws our attention as compared with the classical defect POMs for the following reasons: (1) the $\{WO(H_2O)\}$ linker between two $[B\text{-}\alpha\text{-}AsW_9O_{33}]^{9-}$ could serve as a starting point for rotation and dissociation, which may facilitate the generation of a number of building blocks in solution at different pH values;[12] (2) the stereodirecting influence of the lone pair on the As^{III} atom guarantees the emergence of the lacunary building blocks, resulting in a very different reactivity compared with vacant POMs with tetrahedral hetero groups;[1b] (3) it is easy to prepare the precursor. It is our understanding that several RE-containing arsenotungstates have been isolated based on $[As_2W_{19}O_{67}(H_2O)]^{14-}$ including $[Gd_8As_{12}W_{124}\ O_{432}(H_2O)_{22}]^{60-}$,[10] $[Tb_2(pic)(H_2O)_2(B\text{-}\beta\text{-}AsW_8O_{30})_2(WO_2(pic)_3]^{10-}$,[12] $[Tb_8(pic)_6(H_2O)_{22}(B\text{-}\beta\text{-}AsW_8O_{30})_4(WO_2(pic))_6]^{12-}$,[12] $[Ln_{16}As_{16}W_{164}O_{576}(OH)_8(H_2O)_{42}]^{80-}$,[9c] and $Li_8[Ln_4As_5W_{40}O_{144}(H_2O)_{10}\ (Gly)_2]\cdot 25H_2O$.[13] But, most of the previous reports on RE-containing arsenotungstates are on those that are purely inorganic

[a]*Henan Key Laboratory of Polyoxometalate, Institute of Molecular and Crystal Engineering, College of Chemistry and Chemical Engineering, Henan University, Kaifeng 475004, Henan, China. E-mail: jpwang@henu.edu.cn, jyniu@henu.edu.cn; Fax: (+86) 37123886876*

[b]*College of Chemistry and Chemical Engineering, Engineering Research Center of Functional Material Preparation, Shangqiu Normal University, Shangqiu, 476000 Henan, China*

†Electronic supplementary information (ESI) available: XPRD patterns of **1–6** (Fig. S1); IR spectra of **1–6** (Fig. S2); the UV-vis spectra of **1** (a), **2** (b), **3** (c), **4** (d), **5** (e), **6** (f) with 5×10^{-5} mol L^{-1} in aqueous solution (Fig. S3); the UV-vis spectra of **3** at different pH values (Fig. S4); the χ_M^{-1} *vs.* *T* curves of **1–4** (Fig. S5); the RE–O bond lengths in compounds **1–6** (Table S1). CCDC 987821–987826 for **1–6**. For ESI and crystallographic data in CIF or other electronic format see DOI: 10.1039/c4dt01703j

or containing monocarboxylic ligands (such as glycine, pyridine-2-carboxylic acid), and little work has been devoted to arsenotungstates containing rare earth metals and multicarboxylic ligands simultaneously. Therefore, it is still meaningful and challenging to synthesize new complexes in this family starting from $[As_2W_{19}O_{67}(H_2O)]^{14-}$. Herein, we choose racemic tartaric acid as the polyfunctional bridging ligand on the basis of the following interesting characteristics: (1) among the extensive library of this type of ligand, tartaric acid appears to be largely undeveloped with only a few examples of TM-coordination POMs[14] and no example of RE-containing arsenotungstate has been reported; (2) the carboxylate groups can be completely or partially deprotonated to generate different tartaric acid segments allowing various acidity-dependent coordination modes, which make the ligand polydentate and thus suitable for leading to a strong possibility of constructing novel RE-containing POMs; (3) the tartaric acid is a flexible ligand which can act as hydrogen bond donors and/or hydrogen bond acceptors, favoring the construction of supramolecular structures.

In consideration of the above-mentioned factors, the dilacunary POM $[As_2W_{19}O_{67}(H_2O)]^{14-}$ was utilized as the precursor, and racemic tartaric acid and rare earth cations as the bridging fragments with the purpose of isolating new POM-based complexes *via* the building block approach. Fortunately, when mixing the $[As_2W_{19}O_{67}(H_2O)]^{14-}$ with rare earth cations (Ho^{III}, Er^{III}, Tm^{III}, Yb^{III}, Lu^{III}, Y^{III}) and tartaric acid molecules, we achieved a new series of polytungstoarsenates(III): $K_{13}LiH_4[RE_2(C_4H_4O_6)(C_4H_2O_6)(AsW_9O_{33})]_2{\cdot}28H_2O$ (RE = Ho^{III} (**1**), Er^{III} (**2**), and $K_9LiH_8[RE_2(C_4H_4O_6)(C_4H_2O_6)(AsW_9O_{33})]_2{\cdot}nH_2O$ (RE = Tm^{III} (**3**), n = 35, Yb^{III}(**4**), n = 33, Lu^{III} (**5**), n = 33, Y^{III} (**6**), n = 36).

Results and discussion

Synthesis

The syntheses of compounds **1–6** were achieved from the reaction of $K_{14}[As_2W_{19}O_{67}(H_2O)]$ with chlorate salts of Ho^{III}, Er^{III}, Tm^{III}, Yb^{III}, Lu^{III}, Y^{III} and racemic tartaric acid in a molar ratio of 5 : 12 : 20 in 60 °C aqueous solution under stirring for 1 h. Several variables have been investigated in our work such as pH, organic components and molar ratio *etc.* First, of importance in the preparation of compounds **1–6**, is the introduction of excess tartaric acid. Its presence during the synthesis is crucial because the replacement of tartaric acid by hexane diacid, glutaric acid or succinic acid does not result in the desired product. To the best of our knowledge, tartaric acid as a multidentate oxygen-donor organic ligand is a perfect candidate to investigate the possibility of synthesizing RE-POM cluster species, as it is effective at stabilizing rare earth metals even in high pH aqueous solutions. This essential property has prompted us to explore its effects as a structure directing reagent and one reactant in this reaction system. In fact, other polycarboxylic acids such as malonic acid, hexane diacid, glutaric acid and succinic acid have also been used, and to our regret, we can only obtain some precipitation rather than monocrystal samples, which may be ascribed to their weaker complexation compared to tartaric acid. In addition, if the tartaric acid is added in stoichiometric amounts, some precipitate will form, resulting in the low yield. Therefore, it is supposed that the excess tartaric acid might serve as a buffer and provide a mild environment for the POMs and rare earth metals, preventing them from precipitating. This phenomenon is similar to the citric acid reported by Xu's group.[15] In particular, it is essential for the reaction to be conducted at suitable pH. Parallel experiments confirm that the crystals of compounds **1–6** can just be isolated in the pH range of 5.5–6.5, and the higher the pH is, the lower the yield.

Structural descriptions

Bond valence sum calculations[16] indicate that all W atoms, As atoms and RE atoms in **1–6** are in the +6, +3 and +3 oxidation states, respectively. For each compound of the six, a lithium ion is added based on elemental analysis. In consideration of the balance of the charge state, four hydrogen ions need to be added for **1**, **2** and eight hydrogen ions for **3**, **4** and **5**. The RE–O bond lengths (Table S1 in the ESI†) almost decrease as the ionic radius of the RE^{III} cations decreases, which is in accordance with the effect of the lanthanide contraction. Single crystal X-ray diffraction analyses reveal that compounds **1–6** crystallize in the triclinic space group $P\bar{1}$ and contain similar polyanions $[RE_2(C_4H_4O_6)(C_4H_2O_6)(AsW_9O_{33})]_2^{18-}$ (Fig. 1a), which are connected by K^+ resulting in the 3D framework (Fig. 2). Herein, only a case of compound **1** is illustrated in the following description.

The polyanion of compound **1** is composed of two B-α-$\{AsW_9O_{33}\}$ units opposed to each other, sandwiching a unique cage-like metal–oxide moiety and possessing an "S-shaped" structure, where the cage-like metal–oxide cluster is constituted by four lanthanide cations and four tartaric acid segments. In the cluster, the metal–oxide fragment acting as a bridge connects the two $\{AsW_9O_{33}\}$ units. Subtly, the four rare earth cations of the metal–oxide fragment are in a parallelogram plane (Fig. 1b). Of the four rare earth cations, the two cations located on the same diagonal are crystallographically equivalent and the four rare earth cations are subdivided into two categories: Ho1 and Ho2. The eight-coordinate center Ho1

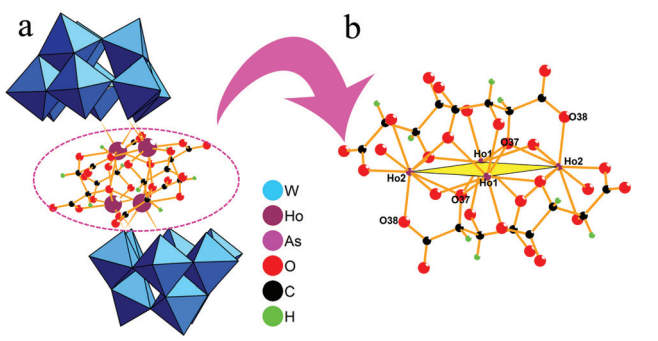

Fig. 1 (a) Polyhedral/ball-and-stick representation of the structural unit of compound **1**; and (b) the metal oxide cluster in compound **1**.

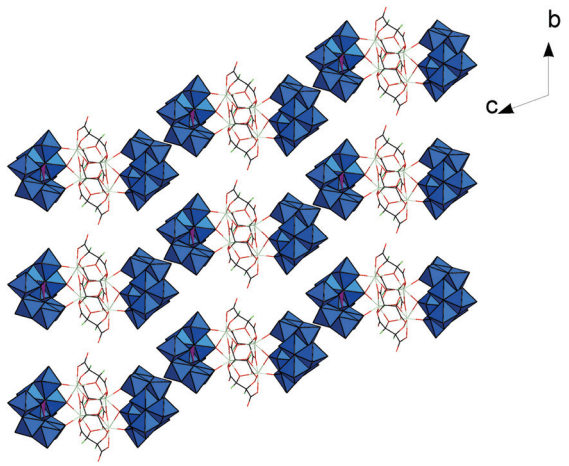

Fig. 2 Packing of the POM in compound **1** viewed along the *a*-axis (K^+ and H_2O are omitted for clarity).

and Ho2 could be considered as the hinges linking the metal–oxide fragment and two$\{AsW_9O_{33}\}$ subunits together *via* two Ho–O(W) bonds and six Ho–O(C) bonds exhibiting a distorted dodecahedral coordination geometry (Ho1–O: 2.219(10)–2.453(11) Å; Ho2–O: 2.271(12)–2.494(11) Å) (Fig. 3). It should be mentioned that the tartaric acid molecules have unusual chelation modes. There are two non-equivalent tartaric acid segments above/below the plane. The first tartaric acid pieces bridge two rare earth ions simultaneously, exploiting an unusual μ_2:μ_2:μ_3:μ_2 fashion, while the other, just like adhesive chelates, bridges three lanthanide ions concurrently, employing μ_3:μ_2:μ_4:μ_2 mode. Or else, μ_4-O37 and μ_2-O38 of the latter tartaric acid are monoprotonated, but no atom is observed as protonated according to bond value calculations. As far as we know, such two coordination modes of the tartrate ligand are seldom reported. In a word, those two uncommon coordination modes may be two key factors in providing the strong complexation between tartaric acid segments and the large metal–oxide framework. And the complexation in turn dictates the configurational stability of the compounds **1–6**.

XRPD and FT-IR patterns

The XRPD patterns for compounds **1–6** are presented in Fig. S1.† The diffraction peaks of simulated patterns do not completely match with experimental patterns because the samples of **1–6** have badly weathered before the XRPD experiments. The differences in the intensity may be due to the preferred orientation of the powder samples.

The peak shapes of the IR spectra in the 400–3500 cm^{-1} region of **1–6** are similar (Fig. S2†), indicating that the polyanions in **1–6** are isostructure. Broad peaks at 3435 cm^{-1} and 1615 cm^{-1} are attributed to the stretching and bending modes of lattice and coordinated water molecules. The peaks at 1395 cm^{-1} may correspond to the vibration of the carboxyl group. The stretching vibration of C–O (RE) may be responsible for the peaks at 1081 cm^{-1}. A characteristic peak for the polyanion at 943 cm^{-1} can be assigned to the W=O stretching vibration and peaks at 889 cm^{-1}, 747 cm^{-1} and 802 cm^{-1} belong to the two types of W–O–W stretching vibrations, and the peak at 703 cm^{-1} can be assigned to the W–O(As) stretch.[13]

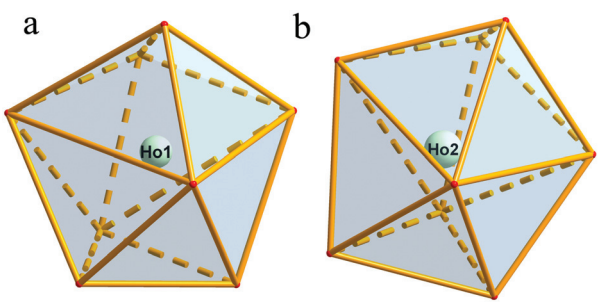

Fig. 3 (a) The coordination environment of the $Ho1^{3+}$; and (b) the coordination environment of the $Ho2^{3+}$.

UV spectra

The UV spectra of compounds **1–6** (5×10^{-5} mol L^{-1}) in aqueous solution display two absorption bands at 200 nm and 250–254 nm (Fig. S3†). The former higher energy band can be assigned to the pπ–dπ charge-transfer transitions of the $O_t \rightarrow W$ band, whereas the latter lower one could be attributed to the pπ–dπ charge-transfer transitions of the $O_{b,c} \rightarrow W$ bands, indicating the formation of polyoxoanions.[17] In order to investigate the stability of the solution of **1–6**, the *in situ* spectroscopic measurements were performed in the aqueous system. Both the position and the strength of the absorption bands of compounds **1–6** do not change, indicating that compounds **1–6** may be stable in the aqueous system at ambient temperature for 5 hours.

It is well known that the POMs are commonly sensitive to the pH value of the studied media. Therefore, in order to investigate the influence of the pH values on the stability of compounds in aqueous solution, **3** has been elaborately probed by means of UV-vis spectra. Diluted HCl solution and LiOH solution were used to adjust the pH values in the acidic direction and in the alkaline direction, respectively. The initial pH value of **3** in water was 4.6. As indicated in Fig. S4,† the UV spectrum of **3** in aqueous solution displays two absorption bands at 200 and 252 nm, and the UV spectrum of **3** does not change at all even when the pH value has been lowered to 1.6. In contrast, when increasing the pH value of **3**, the absorbance band at 252 nm is gradually blue-shifted and becomes weaker and weaker, suggesting the decomposition of the POM skeleton of **3**.[18] This phenomenon is especially obvious when the pH is higher than 9.6, which indicates that the POM skeleton of **3** is destroyed at pH higher than 9.6. The results above reveal that compound **3** could not exist in a solution whose pH is higher than 9.6.

Magnetic properties

Generally speaking, the spin-orbital coupling plays a more important role in the magnetism of lanthanide complexes compared with the crystal field.[19] This spin-orbital coupling leads to the $4f^n$ configuration of Ln^{III} ions, except for Gd^{III}, to split into $^{2S+1}L_J$ states, and the latter further splits into Stark components under the crystal-field perturbation.[19] Thus, the

variable-temperature magnetic properties of a free ion of a metal show strong deviations from the Curie law, and $\chi_M T$ decreases with the cooling temperature because of the depopulation of Stark levels.[20] Although the theory of the paramagnetic properties of lanthanide cations has long been investigated, the presence of the large unquenched orbital angular momentum has not allowed the development of simple models for a rational analysis of the structural magnetic correlations, which makes the analysis of the experimental data more difficult.[20] Herein, variable-temperature magnetic susceptibility measurements of **1–4** have been performed in the range of 1.8–300 K at an applied field of 2 kOe, and the results demonstrate that the magnetic properties of **1–3** are similar while **4** is somewhat different (Fig. 4 and Fig. S5†).

Compounds **1–3** exhibit similar magnetic properties showing antiferromagnetic coupling between lanthanide ions. As an example, only compound **1** is discussed. For compound **1**, the $\chi_M T$ value slowly decreases from 50.35 emu K mol^{-1} at 300 K (Fig. 4a), which is lower than four free Ho^{III}cations (56.67 emu K mol^{-1}, g = 5/4).[20b,c] Once the temperature is lowered to 20 K, the $\chi_M T$ value reduces drastically to 18.34 emu K mol^{-1} at 1.8 K, exhibiting antiferromagnetic coupling with C = 50.89 emu K mol^{-1}, and θ = −6.43 K (Fig. S5a†).

Compound **4** exhibits magnetic properties very different from that of compounds **1–3** as elaborated in Fig. 4d. For compound **4**, at 300 K, the $\chi_M T$ is equal to 10.36 emu K mol^{-1}, which is somewhat higher than the theoretical value of 10.28 emu K mol^{-1} based on four independent Yb^{III} ions with the $^2F_{7/2}$ ground multiplet,[19c,20a] and it almost monotonically decreases to 4.15 emu K mol^{-1} at 1.8 K, suggesting that the depopulation of the Stark levels possibly dominates the magnetic behaviors in compound **4**. As a result, compound **4** does not obey the Curie–Weiss law (Fig. S5d†), which is similar to the compound [Yb$_2$(L)(HL)(NO$_3$)$_6$(HCOO)]·3CH$_3$OH.[20a]

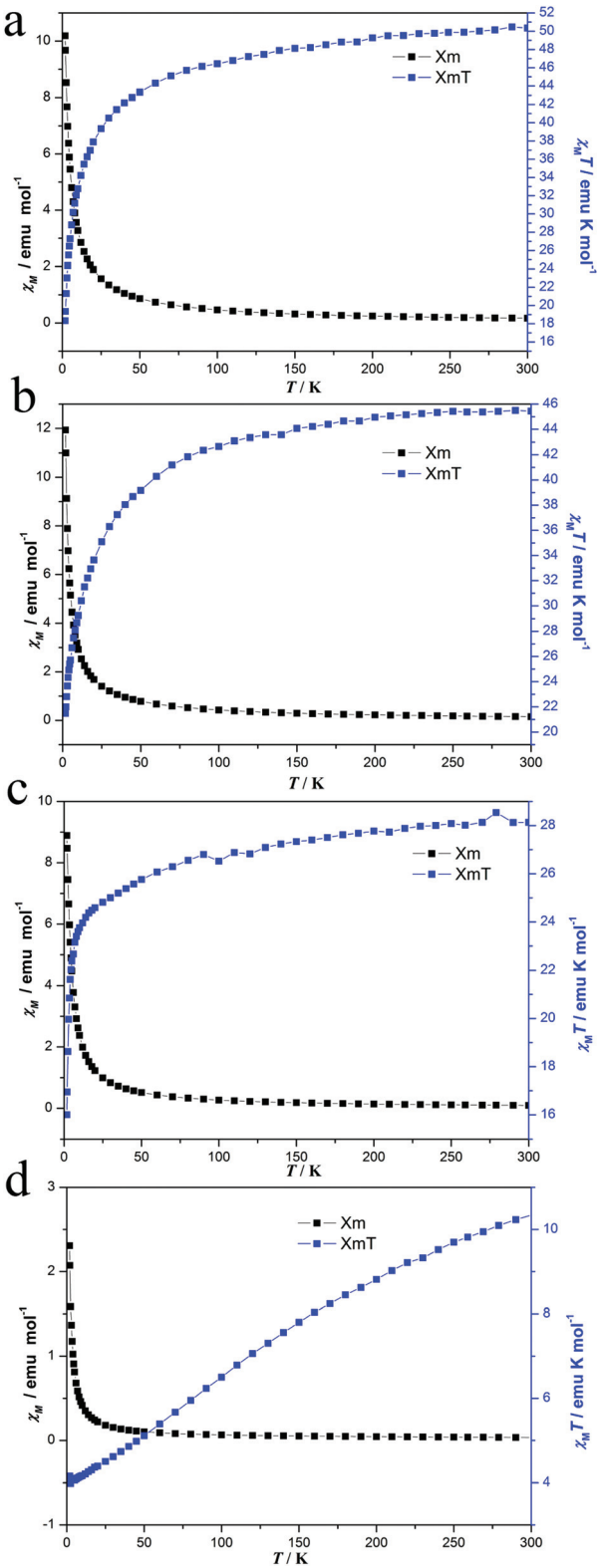

Fig. 4 Plots of χ_M and $\chi_M T$ *vs.* T for **1** (a), **2** (b), **3** (c), **4** (d).

Experimental section

General methods and materials

$K_{14}[As_2W_{19}O_{67}(H_2O)]$ was prepared according to Kortz[9b] and conformed by the IR spectrum. Other chemical reagents were purchased and used without further purification. Elemental analyses (C, H) were conducted on a Perkin-Elmer 2400-II CHNS/O analyzer. IR spectra were recorded on a Bruker VERTEX 70 IR spectrometer using KBr pellets in the range of 4000–400 cm^{-1}. ICP analyses were performed on a Perkin-Elmer Optima 2000 ICP-OES spectrometer. UV-vis absorption spectra were obtained with a U-4100 spectrometer at room temperature. XRPD experiments were performed on a Bruker AXS D8 Advance diffractometer instrument with Cu Kα radiation (λ = 1.54056 Å) in the 2θ = 5–45° range at 293 K. The magnetic data were collected on a Quantum Design SQUID (MPMS-XL7).

Synthesis of $K_{13}H_4Li[Ho_2(C_4H_4O_6)(C_4H_2O_6)(AsW_9O_{33})]_2\cdot 28H_2O$ (1). The representative synthesis of compound **1** was performed as follows: a sample of $K_{14}[As_2W_{19}O_{67}(H_2O)]$ (0.658 g, 0.125 mmol) was added under stirring to a solution of 0.075 g tartaric acid (0.50 mmol) and $HoCl_3\cdot 6H_2O$ (0.30 mmol, 0.114 g) in 15 mL water; ten minutes later, the

pH of the solution was adjusted to about 5.5 with 1.00 mol L^{-1} lithium hydroxide and then the mixture was heated to 60 °C for 1 h. After cooling to room temperature, the clear solution was kept for crystallization. Colorless block crystals were collected after about two weeks. The crystals must be stilled in a capillary tube as they are easy to weather when prepared for X-ray crystal structure determination. Yield: 0.10 g (19.67% based on $HoCl_3{\cdot}6H_2O$). Elemental analysis (%) calcd for **1**: C, 2.83; H, 1.07; K, 7.49; Li, 0.10; Ho, 9.72; As, 2.21; W, 48.76. Found: C, 2.76; H, 1.16; K, 7.61; Li, 0.11; Ho, 9.91; As, 2.23; W, 49.13. Selected IR (KBr, cm^{-1}): 3435 (br), 1615 (s), 1395 (w), 1255 (w), 1202 (w), 1081 (w), 943 (s), 889 (s), 802 (s), 747 (s), 703 (w).

Synthesis of $K_{13}H_4Li[Er_2(C_4H_4O_6)(C_4H_2O_6)(AsW_9O_{33})]_2{\cdot}28H_2O$ (2). The synthesis of **2** is similar to **1** but with $ErCl_3{\cdot}6H_2O$ (0.30 mmol, 0.115 g) instead of $HoCl_3{\cdot}6H_2O$. Yield: 0.09 g (17.68% based on $ErCl_3{\cdot}6H_2O$). Elemental analysis (%) calcd for **2**: C, 2.83; H, 1.07; K, 7.48; Li, 0.10; Er, 9.84; As, 2.20; W, 48.69. Found: C, 2.76; H, 1.20; K, 7.39; Li, 0.11; Er, 10.00; As, 2.16; W, 48.92. Selected IR (KBr, cm^{-1}): 3435 (br), 1613 (s), 1400 (s), 1253 (w), 1209 (w), 1087(w), 940 (s), 890 (s), 801 (s), 742 (s), 698 (w).

Synthesis of $K_9H_8Li[Tm_2(C_4H_4O_6)(C_4H_2O_6)(AsW_9O_{33})]_2{\cdot}35H_2O$ (3). The synthesis of **3** is similar to **1** but with $TmCl_3{\cdot}6H_2O$ (0.30 mmol, 0.115 g) instead of $HoCl_3{\cdot}6H_2O$. Yield: 0.11 g (21.58% based on $TmCl_3{\cdot}6H_2O$). Elemental analysis (%) calcd for **6**: C, 2.84; H, 1.34; K, 5.19; Li, 0.10; Tm, 9.97; As, 2.21; W, 48.83. Found: C, 2.89; H, 1.26; K, 5.15; Li, 0.11; Tm, 9.82; As, 2.14; W, 48.90. Selected IR (KBr, cm^{-1}): 3435 (br), 1610 (s), 1397 (s), 1255 (m), 1209 (w), 1088 (w), 940 (s), 891 (s), 800 (s), 746 (s), 704 (w).

Synthesis of $K_9H_8Li[Yb_2(C_4H_4O_6)(C_4H_2O_6)(AsW_9O_{33})]_2{\cdot}33H_2O$ (4). The synthesis of **4** is similar to **1** but with $YbCl_3{\cdot}6H_2O$ (0.30 mmol, 0.116 g) instead of $HoCl_3{\cdot}6H_2O$. Yield: 0.08 g (15.67% based on $YbCl_3{\cdot}6H_2O$). Elemental analysis (%) calcd for **4**: C, 2.84; H, 1.28; K, 5.21; Li, 0.10; Yb, 10.24; As, 2.22; W, 50.18. Found: C, 2.92; H, 1.17; K, 5.26; Li, 0.10; Yb, 10.18; As, 2.30; W, 49.89. Selected IR (KBr, cm^{-1}): 3435 (br), 1617 (s), 1399 (w), 1255 (w), 1209 (w), 1088 (w), 940 (s), 890 (s), 799 (s), 751 (s), 698 (w).

Synthesis of $K_9H_8Li[Lu_2(C_4H_4O_6)(C_4H_2O_6)_2(AsW_9O_{33})]_2{\cdot}33H_2O$ (5). The synthesis of **5** is similar to **1** but with $LuCl_3{\cdot}6H_2O$ (0.30 mmol, 0.117 g) instead of $HoCl_3{\cdot}6H_2O$. Yield: 0.09 g (17.60% based on $LuCl_3{\cdot}6H_2O$). Elemental analysis (%) calcd for **5**: C, 2.84; H, 1.28; K, 5.20; Li, 0.10; Lu, 10.34; As, 2.22; W, 50.12. Found: C, 2.77; H, 1.30; K, 5.18; Li, 0.11; Lu, 10.43; As, 2.14; W, 49.98. Selected IR (KBr, cm^{-1}): 3435 (br), 1610 (s), 1399 (w), 1255 (s), 1209 (s), 940(s), 890 (s), 799 (s), 747 (s), 697 (w).

Synthesis of $K_9H_8Li[Y_2(C_4H_4O_6)(C_4H_2O_6)(AsW_9O_{33})]_2{\cdot}36H_2O$ (6). The synthesis of **6** is similar to **1** but with $YCl_3{\cdot}6H_2O$ (0.30 mmol, 0.091 g) instead of $HoCl_3{\cdot}6H_2O$. Yield: 0.07 g (14.40% based on $YCl_3{\cdot}6H_2O$). Elemental analysis (%) calcd for **6**: C, 2.97; H, 1.43; K, 5.43; Li, 0.11; Y, 5.49; As, 2.31; W, 51.11. Found: C, 3.04; H, 1.36; K, 5.51; Li, 0.11; Y, 5.39; As, 2.24; W, 51.31. Selected IR (KBr, cm^{-1}): 3435 (br), 1611 (s), 1397 (s), 1253 (s), 1210 (s), 1086 (w), 940 (s), 890 (s), 803 (s), 749 (s), 703 (w).

X-ray crystallography

Single crystal X-ray structure analysis was performed on a Bruker CCD Apex-II diffractometer with Mo Kα radiation (λ = 0.71073 Å) at 296 K. Routine Lorentz polarization and empirical absorption corrections were applied. The structures of compounds **1–6** were solved by direct methods refined by full-matrix least-squares refinements on F^2 using the SHELXL-97 software, and an absorption correction was performed using

Table 1 Crystallographic data for **1–6**

	1	2	3	4	5	6
Formula	$C_{16}H_{72}As_2Ho_4LiK_{13}O_{118}W_{18}$	$C_{16}H_{72}As_2Er_4LiK_{13}O_{118}W_{18}$	$C_{16}H_{90}As_2Tm_4LiK_9O_{125}W_{18}$	$C_{16}H_{86}As_2Yb_4LiK_9O_{123}W_{18}$	$C_{16}H_{86}As_2Lu_4LiK_9O_{123}W_{18}$	$C_{16}H_{92}As_2Y_4LiK_9O_{126}W_{18}$
M_r (g mol^{-1})	6786.58	6795.89	6776.34	6756.72	6764.44	6474.24
T (K)	296(2)	296(2)	296(2)	296(2)	296(2)	296(2)
Crystal system	Triclinic	Triclinic	Triclinic	Triclinic	Triclinic	Triclinic
Space group	$P\bar{1}$	$P\bar{1}$	$P\bar{1}$	$P\bar{1}$	$P\bar{1}$	$P\bar{1}$
a (Å)	11.9933(11)	11.9777(11)	11.939(3)	11.8725(7)	11.879(3)	11.9045(12)
b (Å)	15.2025(13)	15.1643(14)	16.657(4)	16.5529(9)	16.555(4)	16.6180(17)
c (Å)	19.8114(17)	19.7826(18)	17.412(4)	17.2796(10)	17.280(4)	17.4108(17)
α (°)	105.2820(10)	105.2430(10)	98.755(4)	98.6930(10)	98.673(4)	98.786(2)
β (°)	101.371(2)	101.4070(10)	99.642(4)	99.7480(10)	99.747(4)	99.420(2)
γ (°)	107.5420(10)	107.654(2)	90.097(4)	90.1770(10)	90.172(4)	90.080(2)
V ($Å^3$)	3168.6(5)	3149.4(5)	3372.5(13)	3307.0(3)	3308.5(13)	3356.8(6)
Z	1	1	1	1	1	1
D_c (g cm^{-3})	3.549	3.575	3.230	3.302	3.303	3.086
μ (mm^{-1})	19.786	20.059	18.746	19.263	19.405	17.928
Limiting indices	$-14 \le h \le 14$, $-16 \le k \le 18$, $-23 \le l \le 18$	$-14 \le h \le 14$, $-17 \le k \le 18$, $-23 \le l \le 19$	$-14 \le h \le 14$, $-19 \le k \le 14$, $-20 \le l \le 20$	$-14 \le h \le 14$, $-19 \le k \le 19$, $-20 \le l \le 19$	$-14 \le h \le 14$, $-17 \le k \le 19$, $-20 \le l \le 20$	$-14 \le h \le 14$, $-19 \le k \le 19$, $-20 \le l \le 15$
Params	466	466	432	434	439	433
Reflns collected	16 247	16 204	17 329	17 030	17 010	17 081
GOF	1.020	1.004	1.030	1.037	1.036	1.027
R_1, wR_2 [$I > 2\sigma(I)$]	0.0483, 0.1185	0.0401, 0.0990	0.0524, 0.1416	0.0461, 0.1185	0.0480, 0.1269	0.0554, 0.1484
R_1, wR_2 [all data]	0.0671, 0.1294	0.0491, 0.1040	0.0702, 0.1546	0.0600, 0.1270	0.0631, 0.1371	0.0845, 0.1669

the SADABS program.[21] In the final refinement, the W, As, lanthanoid, and K atoms were refined anisotropically; the O and C atoms were refined isotropically. The amount of lithium ions was determined based on elemental analysis results. The hydrogen atoms of the tartaric acid groups were placed in calculated positions and then refined using a riding model. All H atoms on water molecules were directly included in the molecular formula. The crystallographic data for **1–6** are given in Table 1.

Conclusions

In summary, six lanthanoid-based arsenotungstates have been obtained by the building block approach. Furthermore, the magnetic behaviors of **1–4** have been investigated. The work has just proved that the polyanion precursor $[As_2W_{19}O_{67}(H_2O)]^{14-}$ is a superexcellent starting material for the synthesis of elaborate POMs. In the following work, we will introduce different polycarboxylate ligands into the present system and attempt to explore the role of the organic ligands in the reactions.

Acknowledgements

We gratefully acknowledge financial support from the Natural Science Foundation of China (no. 21071042, 21171048, 21172052, 21201116) and the Foundation of Education Department of Henan Province (no. 12A150004 and 14A150028).

Notes and references

1 (*a*) F. Hussain, B. S. Bassil, U. Kortz, O. A. Kholdeeva, M. N. Timofeeva, P. Oliveira, B. Keita and L. Nadjo, *Chem. – Eur. J.*, 2007, **13**, 4733; (*b*) B. S. Bassil and U. Kortz, *Z. Anorg. Allg. Chem.*, 2010, **636**, 2222; (*c*) A. Dolbecq, E. Dumas, C. R. Mayer and P. Mialane, *Chem. Rev.*, 2010, **110**, 6009; (*d*) P. Gouzerh and A. Proust, *Chem. Rev.*, 1998, **98**, 77.

2 (*a*) Y. F. Song and R. Tsunashima, *Chem. Soc. Rev.*, 2012, **41**, 7384; (*b*) D. L. Long, R. Tsunashima and L. Cronin, *Angew. Chem., Int. Ed.*, 2010, **49**, 1736; (*c*) A. Proust, R. Thouvenot and P. Gouzerh, *Chem. Commun.*, 2008, 1837; (*d*) V. Duffort, R. Thouvenot, C. Afonso, G. Izzet and A. Proust, *Chem. Commun.*, 2009, 6062.

3 (*a*) J. T. Rhule, C. L. Hill and D. A. Judd, *Chem. Rev.*, 1998, **98**, 327; (*b*) C. L. Hill, M. S. Weeks and R. F. Schinazi, *J. Med. Chem.*, 1990, **33**, 2767; (*c*) J. Y. Niu, G. Chen, J. W. Zhao, P. T. Ma, S. Z. Li, J. P. Wang, M. X. Li, Y. Bai and B. S. Ji, *Chem. – Eur. J.*, 2010, **16**, 7082.

4 (*a*) M. Sadakane and E. Steckhan, *Chem. Rev.*, 1998, **98**, 219; (*b*) I. M. Mbomekalle, B. Keita, L. Nadio, P. Berthet, K. I. Hardcastle, C. L. Hill and T. M. Anderson, *Inorg. Chem.*, 2003, **42**, 1163.

5 (*a*) A. Müller, F. Peter and M. T. Pope, *Chem. Rev.*, 1998, **98**, 239; (*b*) J.-D. Compain, P. Mialane, A. Dolbecq, I. M. Mbomekallé, J. Marrot, F. Sécheresse, E. Rivière, G. Rogez and W. Wernsdorfer, *Angew. Chem., Int. Ed.*, 2009, **48**, 3077.

6 A. Müller, F. Peters, M. T. Pope and D. Gatteschi, *Chem. Rev.*, 1998, **98**, 239.

7 K. Wassermann, M. H. Dickman and M. T. Pope, *Angew. Chem., Int. Ed.*, 1997, **36**, 1445.

8 A. Müller, E. Beckmann, H. Bögge, M. Schmidtmann and A. Dress, *Angew. Chem., Int. Ed.*, 2002, **41**, 1162.

9 (*a*) N. L. Laronze, M. Haouas, J. Marrot, F. Taulelle and G. Hervé, *Angew. Chem., Int. Ed.*, 2006, **45**, 139; (*b*) U. Kortz, M. G. Savelieff, B. S. Bassil and M. H. Dickman, *Angew. Chem., Int. Ed.*, 2001, **40**, 3384; (*c*) F. Hussain and G. R. Patzke, *CrystEngComm*, 2011, **13**, 53; (*d*) W. L. Chen, Y. G. Li, Y. H. Wang, E. B. Wang and Z. M. Su, *Dalton Trans.*, 2007, 4293.

10 F. Hussain, F. Conrad and G. R. Patzke, *Angew. Chem., Int. Ed.*, 2009, **48**, 9088.

11 M. Sadakane, M. H. Dickman and M. T. Pope, *Angew. Chem., Int. Ed.*, 2000, **39**, 2914.

12 C. Ritchie, E. G. Moore, M. Speldrich, P. Kögerler and C. Boskovic, *Angew. Chem., Int. Ed.*, 2010, **49**, 7702.

13 C. Ritchie, M. Speldrich, R. W. Gable, L. Sorace, P. Kögerler and C. Boskovic, *Inorg. Chem.*, 2011, **50**, 7004.

14 X. K. Fang, T. M. Anderson and C. L. Hill, *Angew. Chem., Int. Ed.*, 2005, **117**, 3606–3610.

15 F. Y. Li, W. H. Guo and L. Xu, *Dalton Trans.*, 2012, **41**, 9220.

16 B. I. D. Brown and D. Altermatt, *Inorg. Chem.*, 1985, **B41**, 244.

17 J. Y. Niu, K. H. Wang, H. N. Chen, *et al.*, *Cryst. Growth Des.*, 2009, **9**, 4362.

18 J. J. Wei, L. Yang, P. T. Ma, J. P. Wang and J. Y. Niu, *Cryst. Growth Des.*, 2013, **13**, 3554.

19 (*a*) J. C. G. Bünzil and C. Piguet, *Chem. Rev.*, 2002, **102**, 1897; (*b*) Y. Li, F. K. Zheng, X. Liu, W. Q. Zou, G. C. Guo, C. Z. Lu and J. S. Huang, *Inorg. Chem.*, 2006, **45**, 6308; (*c*) Z. H. Zhang, T. Okamura, Y. Hasegama, H. Kawaguchi, L. Y. Kong, Y. W. Sun and N. Ueyama, *Inorg. Chem.*, 2005, **44**, 6219; (*d*) W. Huang, D. Y. Wu, P. Zhou, D. Guo, C. Y. Duan and Q. J. Meng, *Cryst. Growth Des.*, 2009, **9**, 1361.

20 (*a*) Z. H. Zhang, Y. Song, T. Okamura, Y. Hasegawa, W. Y. Sun and N. Ueyama, *Inorg. Chem.*, 2006, **45**, 2896; (*b*) J. P. Costes and F. Nicodème, *Chem. – Eur. J.*, 2002, **8**, 3442; (*c*) S. W. Zhang, Y. Wang, J. W. Zhang, P. T. Ma, J. P. Wang and J. Y. Niu, *Dalton Trans.*, 2012, **41**, 3764.

21 (*a*) G. M. Sheldrick, *SHELXS97, Program for Crystal Structure Solution*, University of Göttingen, Göttingen, Germany, 1997; (*b*) G. M. Sheldrick, *SHELXL97, Program for Crystal Structure Refinement*, University of Göttingen, Göttingen, Germany, 1997.

